Journal of Chromatography, 539 (1991) 1–14
Elsevier Science Publishers B.V., Amsterdam

CHROM. 22 844

High-performance liquid chromatography retention index and detection of nitrated polycyclic aromatic hydrocarbons

TYNG-YUN LIU and ALBERT ROBBAT, Jr.*

Trace Analytical Measurement Laboratory, Chemistry Department, Tufts University, Medford, MA 02155 (U.S.A.)

(First received June 6th, 1990; revised manuscript received September 24th, 1990)

ABSTRACT

Based on reversed-phase isocratic experiments and gradient optimization modeling, acetonitrile was found to provide optimum separation of nitrated polycyclic aromatic hydrocarbons (nitro-PAHs). A 31-min linear gradient between 24% and 80% acetonitrile in water at 35°C and 0.5 ml/min flow-rate was established. Nitro-PAH retention indices, *I*, were measured under these conditions. It was found that retention index values varied with changing column temperature and/or mobile phase compositions.

Diode-array, fluorescence (FD) and chemiluminescence (CD) detection were studied for nitro-PAHs. Diode-array detection responded linearly with detection limits between 2 and 12 ng/compound injected. In addition, dual-wavelength UV absorbance ratio (A_{230}/A_{254}, A_{330}/A_{254} and A_{230}/A_{330}) measurements at these wavelength pairs were reported. Fluorescence and chemiluminescence provided increased selectivity and sensitivity. Four orders of magnitude linear range were found for both detection methods with detection limits between 10 and 15 pg and 50 pg (on an NO_2/compound mole basis), respectively.

INTRODUCTION

Over the last decade, much research has been directed toward the development of analytical methodologies for the detection, identification, and quantification of nitrated polycyclic aromatic hydrocarbons (nitro-PAHs). Much of this effort is due to the fact that many nitro-PAHs produce mutagenic as well as carcinogenic activity [1–11]. Moreover, some isomeric nitro-PAHs have been shown to be genotoxic while others have not [1–4,8]. Thus, the requirement that analytical tools be capable of providing isomeric identification is self-evident. To date, total nitro-PAH concentrations found in environmental samples such as aerosols of ambient air; air, diesel exhaust, and wood smoke particulate matter; carbon black; grilled foods such as sausage, chicken, and fish; as well as nitro-PAH metabolites in biological tissue are typically < 10 ppm. This makes identification of isomers extremely difficult requiring well-defined chromatographic operating conditions concomitant with selective detection.

Most nitro-PAH methods have centered on gas chromatography (GC). Principally, this is due to the higher column separation factors achieved with capillary GC and the wide variety of gas-phase, specific detectors that are commercially

0021-9673/91/$03.50 © 1991 Elsevier Science Publishers B.V.

available as compared to high-performance liquid chromatography (HPLC) [12–27]. For example, over fifty nitrated PAHs have been separated and identified with a 25 m × 0.31 mm I.D. fused-silica capillary coated with a 0.25-μm film of SE-52 and detected by an NO·/O_3-specific chemiluminescence detector. Models were developed that both predicted retention characteristics of nitro-PAHs for standards that were not available and for a set of descriptors used to confirm nitro-PAH identity from actual GC retention obtained from a diesel exhaust particulate extract [21–23]. Many publications [12–20] have documented the presence of highly toxic OH–NO_2–PAHs, multi-condensed ring nitro-PAHs, and their metabolites present in the above-mentioned samples. Although capillary GC provides unmatched resolving power compared to HPLC, it is not amenable to thermally labile or low volatility organic compounds. High-resolution HPLC currently provides a sufficient alternative to GC for these types of compounds. Published reports illustrate reversed-phase gradient HPLC with UV, fluorescence, peroxyoxalate and NO·/O_3 chemiluminescence, and electrochemical detection [28–36]. These studies have focused primarily on demonstrating nitro-PAH detector applicability (in particular for 1-nitropyrene) and not on nitro-PAH HPLC retention characteristics.

In a recent paper, the effect of temperature (T) (35–65°C) and organic modifier (acetonitrile, methanol) on the isocratic retention characteristics of nitro-PAHs on a reversed-phase C_{18} column were studied. The log k' (capacity factor) values were linearly dependent on organic–water volume fraction (φ) with plot slopes solvent-dependent. Van 't Hoff plots, log k' *vs.* $1/T$, revealed nitro-PAH transfer between the mobile and stationary phases were organic modifier and volume fraction dependent as well as compound specific [37]. The results from this study in combination with a commercially available software package (DryLab G) for optimizing gradient reversed-phase HPLC conditions were used to generate nitro-PAH retention index values I. Diode-array, fluorescence and chemiluminescence detection under optimum gradient conditions were evaluated, as well as nitro-PAH retention characteristics. The results of this study are presented in this paper.

EXPERIMENTAL

Chemicals and materials

The mobile phase consisted of Milli-Q purified water (Millipore, Milford, MA, U.S.A.) with HPLC-grade acetonitrile and methanol (Fisher Scientific, Medford, MA, U.S.A.) as the organic modifier. The mobile phase was filtered through a 0.45-μm nylon-66 filter (Rainin, Woburn, MA, U.S.A.), ultrasonicated and vacuum degased prior to use. The mobile phase was purged with helium throughout the HPLC experiment. Sources of nitro-PAH compounds have been identified elsewhere [38]. Nitro-PAHs were used without further purification. Standard solutions consisted of *ca.* 1 mg of nitro-PAH in 1 ml of acetonitrile. After preparation, samples were stored in the dark and refrigerated.

HPLC instrumentation

Reversed-phase HPLC separations were performed using a Hewlett-Packard (Palo Alto, CA, U.S.A.) 1090M liquid chromatography system equipped with a DR5 ternary delivery solvent system, diode-array and fluorescence detectors (standard flow

cell), temperature-controlled autosampler and column compartments. The Hewlett-Packard HPLC ChemStation controlled experimental conditions, collected and evaluated retention data as well as UV and fluorescence spectra. Sample injections were made using the autosampler and autoinjector system. A Rheodyne 3 mm × 0.5 μm column inlet filter preceded the analytical column, a 250 × 2.1 mm, 5 μm particle size, octadecylsilane, C_{18}, column (Alltech, Deerfield, IL, U.S.A.). Sample injections were made after the analytical column equilibrated with the mobile phase and the column temperature stabilized (35–55°C). HPLC flow-rate was 0.5 ml/min.

Diode-array UV detection. Chromatographic signals were simultaneously monitored at 230, 254 and 330 nm. Dual-wavelength absorbance ratios for each nitro-PAH were calculated by dividing the peak height measured at λ_1/λ_2, *viz.*, A_{230}/A_{254}, A_{330}/A_{254} and A_{330}/A_{230}. Four nitro-PAHs were used to evaluate the dynamic range and detection limit at 254 nm and 330 nm. The standard solutions, 200 ng/μl of each compound, were serially diluted until analyte signals were no longer observable.

Fluorescence detection. Nitro-PAHs were reduced to their amino analogues by a silica gel–zinc metal mixture (< 200 mesh; 1:1, w/w) contained in a 40 mm × 2.1 mm I.D. stainless-steel tube. The mobile phase consisted of 24% to 80% acetonitrile with 30 m*M* aqueous ammonium acetate (Aldrich, Milwaukee, WI, U.S.A.) solution. Nitro-PAH reduction efficiencies were evaluated in the pre-column derivatization mode, *i.e.*, the reducing column was placed before the analytical column. The conversion yield was calculated by measuring the peak area of unreacted nitro-PAHs with and without catalyst. The stop-flow scanning technique combined with pre-column reduction was used to obtain the optimal pair of excitation/emission ($\lambda_{ex}/\lambda_{em}$) wavelengths by stopping the mobile phase flow and trapping the reduced nitro-PAHs in the flow cell. Excitation and emission spectra were obtained separately to determine optimum $\lambda_{ex}/\lambda_{em}$ wavelength pair for each compound.

Chemiluminescence detection. Details of the $NO\cdot/O_3$ chemiluminescence detection [21,30] and the interface [39] (used to separate the mobile phase from the analyte before the latter reached the detector) have previously been described.

HPLC retention index system

Nitro-PAH retention behavior under varying HPLC operating conditions was evaluated. Retention index, *I*, provides a calculated experimental measurement of solute retention relative to a pair of internal standards:

$$I = 100\,[n + (t_{r(s)} - t_{r(n)})/(t_{r(n+1)} - t_{r(n)})] \quad (1)$$

where $t_{r(s)}$ is the measured solute retention for which *I* is to be calculated, $t_{r(n)}$ and $t_{r(n+1)}$ are the bracketing compound retention times that elute immediately prior to and following the solute, while *n* is the number of rings present in the standard $t_{r(n)}$. The bracketing compounds used in this study were: nitrobenzene, 1-nitronaphthalene, 9-nitroanthracene, 6-nitrochrysene and 6-nitrobenzo[*a*]pyrene. For those compounds that eluted before nitrobenzene, *I* was calculated by dividing $t_{r(s)}$ by $100\cdot t_{r(\text{nitrobenzene})}$. Nitro-PAH retention times were obtained at 254 nm.

DryLab G software (LC Resources, Lafayette, CA, U.S.A.) was used to determine optimum reversed-phase nitro-PAH separation conditions on the C_{18}

column as a function of linear gradient ramp and organic modifier (acetonitrile and methanol). Relative resolution maps and predicted chromatograms were calculated and plotted using this program.

RESULTS AND DISCUSSION

The objective of this paper was to study nitro-PAH retention characteristics under reversed-phase gradient HPLC conditions and to establish their retention indices at optimum experimental conditions. A secondary objective was to demonstrate applicability of these conditions with some nitro-specific detection methods. Toward this end, we reported earlier on the isocratic reversed-phase retention characteristics of nitro-PAHs as a function of organic modifier (acetonitrile and methanol), volume fraction (50:50, 60:40 and 70:30, v/v) and temperature (35–55°C). It was found that under optimum conditions, many of the nitro-PAHs exceeded "practical" analytical elution times (>1 h) with k' values greater than 10. For the purposes of this study, advantage was taken of the linear relationships found between log k' and φ to predict the optimum organic modifier for gradient separation of nitro-PAHs. The relative variation in S between each solvent type over the entire data set should provide the mechanism for such prediction. (S is the slope value for the log k' *vs.* φ plot and is related to the solvent strength of the organic modifier in the mobile

TABLE I

RELATIVE VARIATION IN S VALUES ($S=\delta S/S_{av}$) AS A FUNCTION OF ACETONITRILE–WATER AND METHANOL–WATER COMPOSITIONS

See ref. 37 for experimental data. Notes: (1) nitro-PAH retention times exceeded 1.5 h for compounds 38, 39, 43, 44 and 45 in methanol–water mobile phase compositions; (2) the remaining compounds listed in Table II were not studied; (3) $\delta S/S_{av}$ values were calculated by subtracting S_{exp} (slope of log k' *vs.* φ) from S_{cal} (calculated from S *vs.* log k_0 plots) divided by $100 \cdot S_{av}$ (average experimental S value for the corresponding compounds in a given solvent system).

No.	$\delta S/S_{av}$		No.	$\delta S/S_{av}$	
	Acetonitrile	Methanol		Acetonitrile	Methanol
2	− 2.23	1.58	23	− 5.77	6.58
3	8.21	− 3.44	24	3.40	−0.33
4	10.45	− 1.95	25	− 7.09	5.81
7	3.38	− 0.33	27	− 4.96	1.00
9	1.21	5.69	28	− 1.58	−0.68
10	0.79	− 2.77	29	− 9.33	7.19
11	−16.30	3.11	30	2.01	−7.22
12	0.74	0.18	31	− 3.54	−1.23
14	6.53	− 3.73	33	6.59	−5.03
15	− 9.30	6.44	34	− 2.28	2.18
16	5.13	−13.35	35	2.11	−7.60
17	−12.29	3.22	38	− 3.24	
18	− 0.23	3.00	39	12.65	
19	−12.15	− 0.22	43	8.78	
20	3.50	− 1.25	44	22.61	
21	− 7.43	− 0.24	45	9.22	

TABLE II

NITRATED POLYCYCLIC AROMATIC HYDROCARBONS

No.	Compound	No.	Compound
1	4-Nitroquinoline-N-oxide	24	1-Nitro-2-methylnaphthalene
2	8-Nitroquinoline	25	2,7-Dinitrofluorene
3	6-Nitroquinoline	26	2,8-Dinitrodibenzothiophene
4	5-Nitroquinoline	27	4-Nitrobiphenyl
5	Nitrobenzene	28	3-Nitrobiphenyl
6	2,4,5,7-Tetranitro-9-fluorenone	29	2,2'-Dinitrobenzyl
7	5-Nitro-6-methylquinoline	30	3-Nitrodibenzofuran
8	8-Nitro-7-methylquinoline	31	2-Nitrofluorene
9	1,8-Dinitronaphthalene	32	2-Nitrodibenzothiophene
10	1,3-Dinitronaphthalene	33	9-Nitrophenanthrene
11	2,4,7-Trinitro-9-fluorenone	34	9-Nitroanthracene
12	1,5-Dinitronaphthalene	35	3-Nitrophenanthrene
13	2,2'-Dinitrobiphenyl	36	1,3-Dinitropyrene
14	1-Nitronaphthalene	37	1,6-Dinitropyrene
15	1,3,6,8-Tetranitronaphthalene	38	1-Nitropyrene
16	9,10-Dinitroanthracene	39	3-Nitrofluoranthene
17	2,7-Dinitro-9-fluorenone	40	1,8-Dinitropyrene
18	2-Nitro-9-fluorenone	41	7-Nitro-3,4-benzocoumarin
19	2,6-Dinitro-9-fluorenone	42	4-Nitro-*p*-terphenyl
20	2-Nitronaphthalene	43	6-Nitrochrysene
21	3-Nitro-9-fluorenone	44	3-Nitroperylene
22	5-Nitroindan	45	6-Nitrobenzo[*a*]pyrene
23	2-Nitrobiphenyl		

phase; k' is the nitro-PAH capacity factor and φ the volume fraction of the organic modifier). The relative variation of S, ($\delta S/S_{ave}$), was calculated from S_{exp} from the slope of log k' *vs.* φ plots, minus S_{cal} from S *vs.* log k_0 (k' at 100% H_2O) plots, divided by the average S_{exp} for each solvent type times one hundred. (See Tables II and VI in ref. 37 for details). The results of the $\delta S/S_{av}$ calculation for both organic modifiers are summarized in Table I (see Table II for compound No. and identity). As anticipated, acetonitrile was predicted to provide optimum solvent type for gradient nitro-PAH separation in general, evidenced by the wider $\delta S/S_{av}$ compound variations as compared to methanol.

In order to substantiate these findings and to reduce development time, a computer program (DryLab G) capable of calculating relative peak resolution under differing gradient conditions was employed. Twenty-two model compounds were selected representing a wide range of nitro-PAHs. Two experiments were performed for each solvent type linearly programmed between 5 and 100% organic modifier in water at 30 and 90 min, respectively. The flow-rate through the column was 0.5 ml/min. Table III denoted the retention times obtained and bands where peak valleys exceeded 50% (resolution, $R_s < 1.1$). Plots of the relative band resolution for each organic modifier as a function of gradient time suggested an optimum linear mobile phase program of 24% to 80% acetonitrile in water in 31 min. The operating conditions were established after simulation to reduce the overall elution time by decreasing the gradient range (*i.e.*, from 5–100% acetonitrile to 24–80% acetonitrile)

TABLE III

NITRO-PAH RETENTION TIMES

Separation conditions: 5% to 100% organic solvent in water in 30 and 90 min, respectively, at 35°C and 0.5 ml/min flow-rate.

No.	Acetonitrile		Methanol	
	30 min	90 min	30 min	90 min
3	11.63	19.68	12.77	21.25
4	12.82	23.42	14.39	28.03
7	14.62	28.23	17.29	36.40
8	15.03	30.02	18.28	39.30
9	16.23	33.85	19.89	44.22
12	17.68	37.72	20.92	46.20
14	18.28	39.02	22.25[b]	50.12
20	18.73[a]	40.28	22.25[b]	51.57
23	19.10[a]	42.21	22.68	55.85[a]
24	19.85[a]	44.05	23.75	56.18[a]
25	19.92[a]	45.23	24.70	58.80
27	20.58	46.19	25.73	61.82
31	21.24	47.88	26.35	63.99
33	21.89	49.75	27.21	66.85
34	22.17[a]	50.55	28.29[a]	68.82
35	22.56[a]	51.97	28.60[a]	69.88
37	23.30[a]	53.77	28.92[a]	70.99
38	23.72[a]	54.30	29.61[a]	73.32
42	24.79	58.12	29.99[a]	74.62
43	25.23	59.02	30.76[b]	78.51[b]
44	26.89	63.47	30.89[b]	78.51[b]
45	27.21	64.49	30.76[a]	89.50

[a] Indicating band pairs where more than 50% valley was found.
[b] Indicating that two nitro-PAH compounds coeluted.

while maintaining gradient slope. The gradient program yielded a minimum resolution compared to all other model compounds for band pair 33/34, *viz.*, $R_s = 1.9$. Table IV illustrated retention time reproducibility and the percent difference between experimental and predicted retention times at optimum gradient conditions (see Fig. 1 for band spacing comparisons; R_s for 33/34 and 42/43 were 2.1 and 1.7, respectively).

Evident from Table III and supported by chromatographic modelling and simulation was the relatively poorer peak resolutions obtained for the model compounds with methanol–water. For example, the maximum resolution for the most poorly resolved band pair was less than 0.13 for band pairs 43/44 as might be expected from Table II findings.

High back pressures were observed at 25°C for volume fractions less than 60% organic with the narrow bore C_{18} column. The high back pressure effectively restricted the useful gradient profile working range for study. Increasing the column temperature resulted in much earlier elution of the model compounds. For example, compound 45 eluted at 31.2 min (35°C) *versus* 28.6 min (55°C) concomitant with coelution of compounds 24/25 and 42/43 with acetonitrile–water mobile phase conditions.

TABLE IV

EXPERIMENTAL AND PREDICTED RETENTION TIMES

Separation conditions: 31-min gradient from 24% to 80% acetonitrile in water at 35°C and 0.5 ml/min flow-rate. Experimental and predicted chromatograms were shown in Fig. 1.

No.	Retention time (min) ± S.D.		
	Experimental ($n=3$)	Predicted	% Difference
3	6.64 ± 0.01	5.94	11.8
4	7.98 ± 0.02	7.54	5.8
7	10.45 ± 0.02	10.28	1.7
8	11.06 ± 0.02	11.01	0.5
9	13.10 ± 0.02	13.06	0.3
12	15.38 ± 0.03	15.43	0.3
14	16.23 ± 0.02	16.33	0.6
20	16.96 ± 0.03	17.09	0.8
23	17.76 ± 0.02	17.93	1.0
24	18.98 ± 0.02	19.13	0.8
25	19.47 ± 0.04	19.51	0.2
27	20.15 ± 0.03	20.38	1.1
31	21.18 ± 0.04	21.45	1.3
33	22.26 ± 0.04	22.56	1.3
34	22.73 ± 0.04	23.04	1.4
35	23.49 ± 0.06	23.79	1.3
37	24.64 ± 0.05	24.96	1.3
38	25.12 ± 0.10	25.49	1.5
42	27.50 ± 0.02	27.53	0.1
43	27.92 ± 0.02	28.18	0.9
44	30.62 ± 0.02	30.92	1.0
45	31.19 ± 0.02	31.50	1.0

Increasing column temperature lessened optimum resolution between band pairs to point where it made little sense for analytical applications. In contrast, relative separation remained the same along with reduced elution times when 10% methanol was added to the acetonitrile–water gradient. For example, compound 45 eluted at 27.5 min as compared to 31.2 min for the binary system.

Retention index experiments were performed for Table II nitro-PAHs. Listed in Table V are the retention index values when the 24% to 80% acetonitrile in water gradient was employed at 35°C, 45°C and at 35°C with a constant 10% methanol added. It was apparent that index values varied greatly as a function of HPLC operating conditions. The amount that a particular I value differed between operating conditions depended largely on the competitive differences in the interactions between the bracketing compounds *and* the target compound with the mobile phase.

Experiments were performed to evaluate three HPLC nitro-specific detection methods. Figs. 1 and 2 illustrate typical diode-array detection responses for the model compounds at 254 nm as well as 230 and 330 nm, respectively. Although nitro-PAH detection limits were wavelength-dependent and moderate (2 to 12 ng injected; signal-to-noise ratio 3:1), dual-wavelength absorbance ratio measurements (see Table VI) can be used for compound identification at the concentration levels found for the

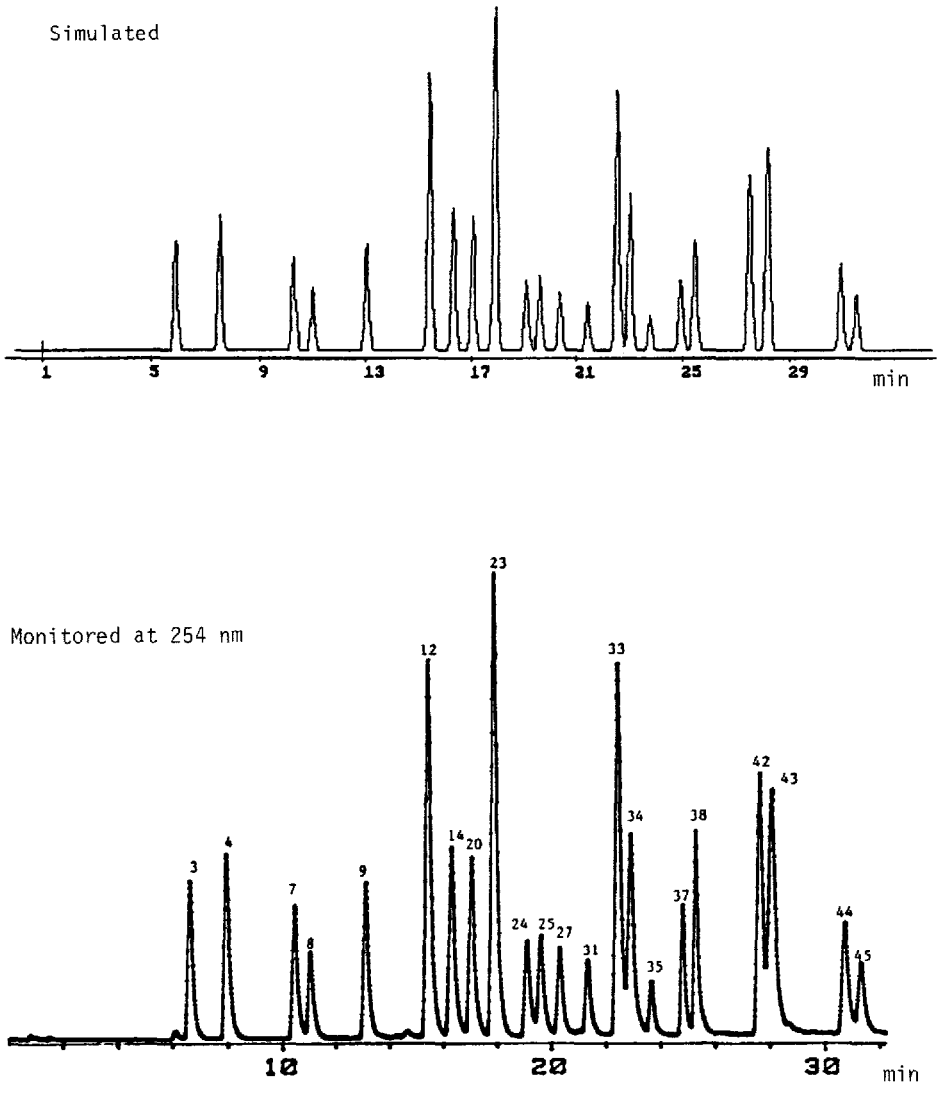

Fig. 1. Simulated and experimental (at 254 nm) chromatograms.

most prevalent nitro-PAHs in environmental samples, *e.g.*, 1-nitropyrene, 1-nitronaphthalene, 2-nitrofluorene. Advantage of UV spectra and chromatographic peak signal superimposition at the three wavelengths, respectively, provided differentiation between closely eluting compounds.

Post-column fluorescence detection was evaluated employing a 4 cm × 2.1 mm reducer column containing a zinc–silica gel (1:1, w/w) mixture. Ammonium acetate (30 m*M*) was added to the acetonitrile–water mobile phase to ensure quantitative

TABLE V

RETENTION INDEX, *I*, OF NITRO-PAHs ± S.D. ($n=3$)

Conditions: (A) 31-min linear gradient between 24 and 80% acetonitrile in water at 0.5 ml/min flow-rate and 35°C; (B), as (A) except 45°C; (C), as (A) except 10% methanol added.

No.	*I*		
	Conditions A	Conditions B	Conditions C
1	57.90 ± 0.16	55.90 ± 0.16	61.20 ± 0.13
2	78.96 ± 0.17	81.52 ± 0.10	76.92 ± 0.31
3	94.82 ± 0.22	99.16 ± 0.27	96.28 ± 0.32
4	95.73 ± 0.21	99.20 ± 0.23	99.31 ± 0.15
5	100.00 ± 0.00	100.00 ± 0.00	100.00 ± 0.00
6	109.30 ± 0.24	117.08 ± 0.26	104.79 ± 0.21
7	126.12 ± 0.21	126.39 ± 0.21	121.39 ± 0.27
8	133.85 ± 0.24	138.34 ± 0.24	134.03 ± 0.28
9	159.97 ± 0.30	158.34 ± 0.30	152.57 ± 0.24
10	185.27 ± 0.18	172.93 ± 0.18	174.61 ± 0.26
11	187.89 ± 0.23	179.90 ± 0.22	184.01 ± 0.31
12	189.08 ± 0.23	181.29 ± 0.34	187.11 ± 0.28
13	190.95 ± 0.04	188.44 ± 0.04	189.50 ± 0.30
14	200.00 ± 0.00	200.00 ± 0.00	200.00 ± 0.00
15	202.49 ± 0.10	204.17 ± 0.10	201.16 ± 0.32
16	205.34 ± 0.59	206.31 ± 0.57	207.57 ± 0.37
17	205.49 ± 0.10	206.34 ± 0.09	210.43 ± 0.32
18	210.43 ± 0.11	208.29 ± 0.28	211.42 ± 0.25
19	210.80 ± 0.30	208.29 ± 0.28	211.45 ± 0.43
20	211.24 ± 0.34	210.73 ± 0.34	212.15 ± 0.32
21	216.55 ± 0.28	216.27 ± 0.28	216.13 ± 0.29
22	219.02 ± 0.11	219.35 ± 0.11	219.34 ± 0.22
23	223.56 ± 0.29	224.79 ± 0.29	219.78 ± 0.33
24	242.20 ± 0.31	242.57 ± 0.32	240.33 ± 0.36
25	249.84 ± 0.57	248.41 ± 0.37	250.98 ± 0.33
26	257.91 ± 0.03	254.84 ± 0.03	259.55 ± 0.13
27	260.23 ± 0.39	255.07 ± 0.39	259.92 ± 0.34
28	261.85 ± 0.13	258.57 ± 0.10	260.19 ± 0.34
29	269.71 ± 0.11	260.42 ± 0.39	265.84 ± 0.35
30	271.12 ± 0.32	271.78 ± 0.34	274.46 ± 0.08
31	276.06 ± 0.11	275.59 ± 0.13	277.34 ± 0.36
32	283.13 ± 0.03	281.61 ± 0.03	284.59 ± 0.06
33	292.77 ± 0.05	292.83 ± 0.05	294.00 ± 0.32
34	300.00 ± 0.00	300.00 ± 0.00	300.00 ± 0.00
35	309.89 ± 0.27	297.04 ± 0.37	312.33 ± 0.09
36	314.57 ± 0.41	314.05 ± 0.42	318.67 ± 0.38
37	336.82 ± 0.37	337.94 ± 0.03	340.85 ± 0.37
38	346.01 ± 0.23	346.51 ± 0.24	347.66 ± 0.42
39	347.70 ± 0.03	337.47 ± 0.03	348.56 ± 0.21
40	349.23 ± 0.17	337.39 ± 0.17	353.14 ± 0.04
41	390.82 ± 0.08	378.39 ± 0.08	390.17 ± 0.15
42	391.93 ± 0.24	393.49 ± 0.24	390.90 ± 0.23
43	400.00 ± 0.00	400.00 ± 0.00	400.00 ± 0.00
44	482.45 ± 0.19	479.43 ± 0.19	484.23 ± 0.29
45	500.00 ± 0.00	500.00 ± 0.00	500.00 ± 0.00

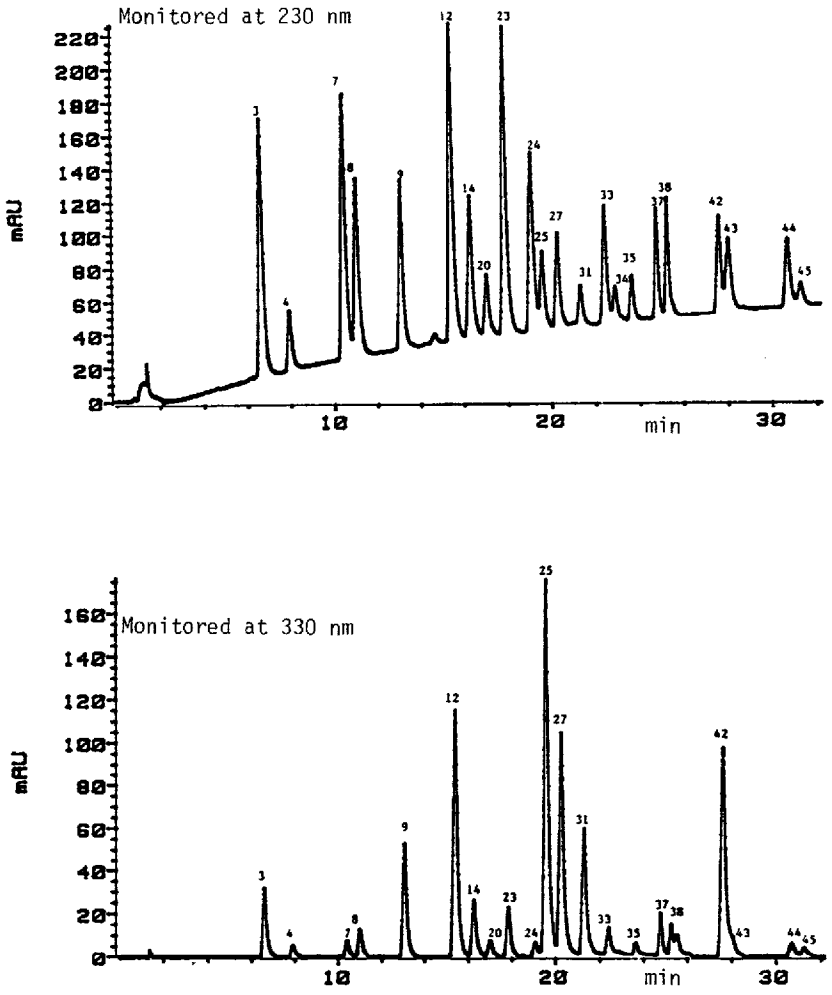

Fig. 2. Typical diode-array detection responses at 230 nm and 330 nm.

conversion (> 99%) of nitro-PAHs to the corresponding amino analogues. Fig. 3 illustrates the fluorescence response for the model compounds at 260/430 nm ($\lambda_{ex}/\lambda_{em}$). It was evident that compared to diode-array detection, fluorescence detection provided much better selectivity and sensitivity. The fluorescence dynamic range spanned four orders of magnitude for most of the model compounds with minimum detectable quantities between 10 and 15 pg of compound injected (see Table VII). Shown in Table VIII are the excitation and emission wavelengths for twenty-six nitro-PAHs (see ref. 35 for the remaining 19 nitro-PAHs).

Lastly, it was demonstrated that gas phase NO · /O_3-specific chemiluminescence detection can be employed with acetonitrile-water mobile phase compositions

TABLE VI

DUAL-WAVELENGTH ABSORBANCE RATIO VALUES FOR NITRO-PAHs ± S.D. ($n=3$)

ND = At least one signal not detected (100 ng/μl compound injected) at the indicated wavelength pair.

No.	A_{230}/A_{254}	A_{330}/A_{254}	A_{230}/A_{330}
1	0.776 ± 0.002	0.306 ± 0.001	2.536 ± 0.010
2	3.481 ± 0.153	0.792 ± 0.002	4.395 ± 0.023
3	0.769 ± 0.002	0.111 ± 0.001	6.928 ± 0.048
4	1.936 ± 0.012	1.860 ± 0.004	1.041 ± 0.002
5	0.375 ± 0.002	ND	ND
6	0.535 ± 0.004	ND	ND
7	4.174 ± 0.056	0.216 ± 0.004	19.324 ± 0.090
8	4.492 ± 0.031	0.566 ± 0.011	7.936 ± 0.035
9	2.544 ± 0.084	1.359 ± 0.008	1.872 ± 0.034
10	0.807 ± 0.004	0.163 ± 0.000	4.951 ± 0.012
11	1.244 ± 0.014	1.190 ± 0.011	1.045 ± 0.002
12	1.890 ± 0.023	1.216 ± 0.003	1.554 ± 0.015
13	1.175 ± 0.002	0.263 ± 0.000	4.468 ± 0.008
14	1.676 ± 0.038	0.545 ± 0.003	3.075 ± 0.050
15	0.854 ± 0.003	0.019 ± 0.000	44.948 ± 0.241
16	ND	0.121 ± 0.005	ND
17	0.893 ± 0.004	0.416 ± 0.004	2.129 ± 0.004
18	0.969 ± 0.002	ND	ND
19	0.978 ± 0.003	0.407 ± 0.001	2.404 ± 0.007
20	0.822 ± 0.004	0.173 ± 0.000	4.751 ± 0.023
21	0.568 ± 0.021	0.103 ± 0.002	5.515 ± 0.040
22	1.856 ± 0.009	1.200 ± 0.001	1.547 ± 0.012
23	1.566 ± 0.011	0.192 ± 0.002	8.114 ± 0.015
24	3.746 ± 0.100	0.271 ± 0.003	13.823 ± 0.213
25	1.872 ± 0.036	7.237 ± 0.004	0.259 ± 0.004
26	0.572 ± 0.003	ND	ND
27	2.569 ± 0.052	4.736 ± 0.049	0.542 ± 0.006
28	0.639 ± 0.002	0.049 ± 0.000	13.041 ± 0.041
29	1.011 ± 0.004	0.171 ± 0.000	5.912 ± 0.023
30	1.791 ± 0.013	2.873 ± 0.061	0.623 ± 0.011
31	1.325 ± 0.011	3.178 ± 0.042	0.417 ± 0.003
32	1.102 ± 0.001	ND	ND
33	0.767 ± 0.002	0.127 ± 0.001	6.039 ± 0.031
34	0.443 ± 0.006	ND	1.073 ± 0.009
35	0.457 ± 0.000	0.413 ± 0.002	21.762 ± 0.002
36	2.061 ± 0.043	0.021 ± 0.001	3.412 ± 0.050
37	2.007 ± 0.019	0.604 ± 0.002	7.017 ± 0.067
38	1.406 ± 0.012	0.286 ± 0.003	ND
39	1.532 ± 0.011	0.233 ± 0.020	5.560 ± 0.010
40	1.068 ± 0.043	0.312 ± 0.005	3.423 ± 0.082
41	0.877 ± 0.000	1.489 ± 0.003	0.589 ± 0.001
42	0.887 ± 0.001	1.499 ± 0.001	0.592 ± 0.001
43	0.728 ± 0.004	ND	ND
44	1.411 ± 0.015	0.196 ± 0.000	7.199 ± 0.025
45	0.770 ± 0.004	0.230 ± 0.000	3.348 ± 0.0.17

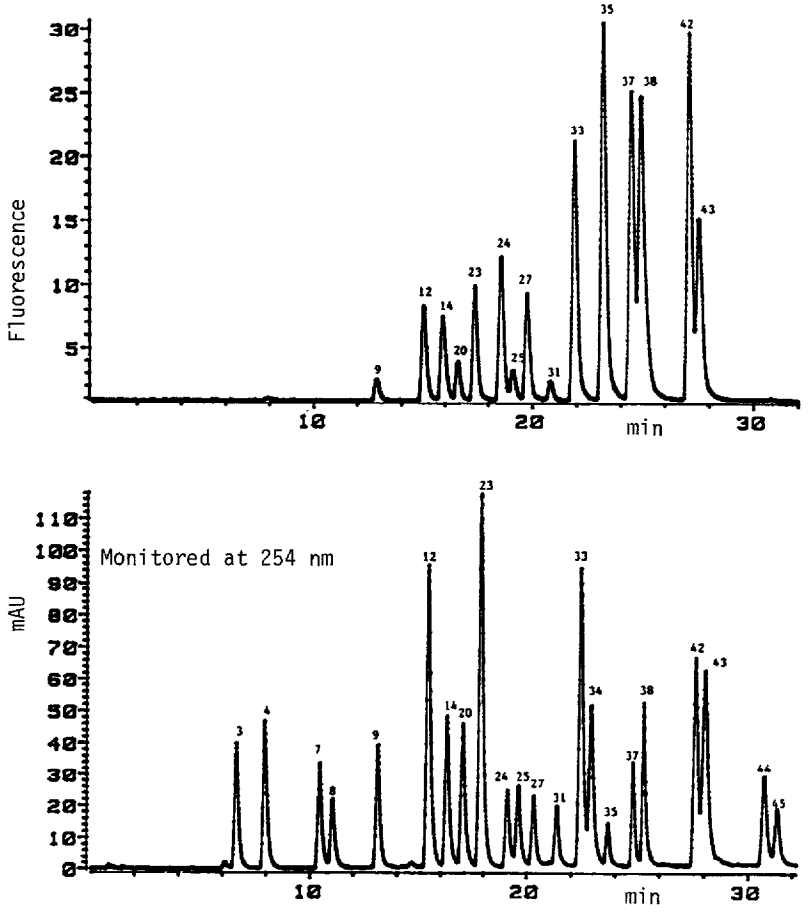

Fig. 3. Fluorescence detection responses at 260/430 nm ($\lambda_{ex}/\lambda_{em}$).

TABLE VII

FLUORESCENCE DETECTION LINEAR DYNAMIC RANGE AND MINIMUM DETECTABLE AMOUNTS

DL = Minimum detectable amount.

Compound	Intercept	Slope	Correlation	DL (pg)
1-Nitronaphthalene	−0.21	3.55	0.999	10
2-Nitrofluorene	0.38	1.54	0.999	15
9-Nitroanthracene	0.17	0.51	0.999	15
1-Nitropyrene	0.33	0.59	0.999	10

TABLE VIII

EXCITATION AND EMISSION WAVELENGTHS FOR NH_2-PAH ANALOGUES

No.	$\lambda_{ex}/\lambda_{em}$ (nm)	No.	$\lambda_{ex}/\lambda_{em}$ (nm)
2	245/432	22	232/350
3	245/432	23	227/394
4	230/485	24	244/414
7	245/490	25	292/387
8	245/432	26	231/407
9	229/417	27	285/367
10	247/420	28	232/399
13	228/372	29	230/335
15	264/417	30	227/359
16	264/495	31	285/370
17	232/387	32	243/407
18	290/365	33	247/430
19	232/387	42	295/425
21	245/407	44	227/540

[30]. Chemiluminescence detection responded linearly (between 70 and 1000 ng/compound injected) *and* on a per mole of NO_2 per mole of compound basis. It was shown that the chemiluminescence detection limit was both volume-fraction dependent as well as flow-rate dependent presumably due to pressure variations within the reaction chamber relative to the $NO \cdot /O_3$ reaction. An interface specifically designed to separate solvent-from-analyte before the latter reached the detector had been demonstrated for nitro-PAHs [39]. For the compounds evaluated, the HPLC–interface–chemiluminescence detection yielded nitro-PAH linear dynamic ranges comparable to the GC–chemiluminescence detection [21] with minimum detection levels of *ca.* 50 pg/compound injected; resulting in two orders of magnitude greater sensitivity than HPLC-chemiluminescence detection.

The gradient system described above, the HPLC- and GC-derived nitro-PAH retention indexes (and GC retention prediction models) in combination with nitro-specific detection capability should provide unparalleled capability for the identification and quantification of nitro-PAHs in complex environmental samples.

ACKNOWLEDGEMENTS

The authors thank Hewlett-Packard company (Palo Alto, CA, U.S.A.) for providing the 1090M HPLC system through their university grants program and LC Resources Inc. (Lafayette, CA, U.S.A.) for DryLab G software.

REFERENCES

1 H. S. Rosenkranz and R. Mermelstein, *Mutat. Res.*, 114 (1983) 217.
2 T. Hirayama, T. Watanabe, M. Akita, S. Shimomura, Y. Fujioka, S. Ozasa and S. Fukui, *Mutat. Res.*, 209 (1988) 67.
3 P. P. Fu, M. W. Chou, D. W. Miller, G. L. White, R. H. Heflich and F. A. Beland, *Mutat. Res.*, 143 (1985) 173.

4 M. W. Chou, R. H. Heflich, D. A. Casciano, D. W. Miller, J. P. Freeman, F. E. Evans and P. P. Fu, *J. Med. Chem.*, 27 (1984) 1156.
5 E. C. McCoy and H. S. Rosenkranz, *Cancer Lett.*, 15 (1982) 9.
6 K. E. Richardson, P. P. Fu and C. E. Cerniglia, *J. Toxicol. Environ. Health*, 23 (1988) 527.
7 A. M. Dietrich, C. R. Guenat, K. B. Tomer and L. M. Ball, *Carcinogenesis*, 9 (1988) 2113.
8 J. R. Thornton-Manning, W. L. Campbell, B. S. Hass, J. J. Chen, P. P. Fu, C. E. Cerniglia and R. H. Heflich, *Environ. Mol. Mutagen.*, 13 (1989) 203.
9 K. El-Bayoumy, S. S. Hecht and D. Hoffmman, *Cancer Lett.*, 16 (1982) 333.
10 H. Ohgaki, N. Matsukura, K. Morino, T. Kawachi, T. Sugimura, K. Morita, H. Tokiwa and T. Hirota, *Cancer Lett.*, 15 (1982) 1.
11 M. Hirose, M. S. Lee, C. Y. Wang and C. M. King, *Cancer Res.*, 44 (1984) 1158.
12 T. Ramdahl, B. Zielinska, J. Arey, R. Atkinson, A. M. Winer and J. N. Pitts, Jr., *Nature (London)*, 321 (1986) 425.
13 R. Kamens, D. Bell, A. M. Dietrich, J. Perry, R. Goodman, L. Claxton and S. B. Tejada, *Environ. Sci. Technol.*, 19 (1985) 63.
14 J. Arey, B. Zielinska, R. Atkinson and A. W. Winer, *Atmos. Environ.*, 21 (1987) 1437.
15 J. Arey, B. Zielinska, R. Atkinson, A. W. Winer, T. Ramdahl and J. N. Pitts, Jr., *Atmos. Environ.*, 20 (1986) 2339.
16 B. Zielinska, J. Arey, R. Atkinson and A. M. Winer, *Atmos. Environ.*, 23 (1989) 223.
17 B. Zielinska, J. Arey, R. Atkinson and P. A. McElory, *Environ. Sci. Technol.*, 23 (1989) 723.
18 B. Zielinska, J. Arey, R. Atkinson and P. A. McElory, *Environ. Sci. Technol.*, 22 (1988) 1044.
19 M. G. Nishioka, C. C. Howard, D. A. Contos, L. M. Ball and J. Lewtas, *Environ. Sci. Technol.*, 22 (1988) 908.
20 M. C. Paputa-Peck, R. S. Marano, D. Schuetzle, T. L. Riley, C. V. Hampton, T. J. Prater, L. M. Skewes, P. H. Ruehle, L. C. Bosch and W. P. Duncan, *Anal. Chem.*, 55 (1983) 1946.
21 A. Robbat, Jr., N. P. Corso, P. J. Doherty and M. H. Wolf, *Anal. Chem.*, 55 (1986) 2078.
22 A. Robbat, Jr., N. P. Corso, P. J. Doherty and D. Marshall, *Anal. Chem.*, 58 (1986) 2072.
23 A. Robbat, Jr., P. J. Doherty, R. M. Hoes and C. M. White, *Anal. Chem.*, 56 (1984) 2697.
24 A. L. Lafleur and K. L. Mills, *Anal. Chem.*, 53 (1981) 1202.
25 J. H. Phillips, R. J. Coraor and S. R. Prescott, *Anal. Chem.*, 55 (1983) 889.
26 W. C. Yu, D. H. Fine, K. S. Chiu and K. Biemann, *Anal. Chem.*, 56 (1984) 1158.
27 B. A. Tomkins, R. S. Brazell, M. E. Roth and V. H. Ostrum, *Anal. Chem.*, 56 (1984) 781.
28 Z. Jin, S. Dong, Y. Li, W. Xu and X. Xu, *Huanjing Huaxue*, 7 (1988) 28.
29 H. S. Rosenkranx, E. C. McCoy, D. R. Sanders, M. Butler, D. K. Kiriazides and R. Mermelstein, *Science (Washington, D.C.)*, 209 (1980) 1039.
30 A. Robbat, Jr., N. P. Corso and T. Y. Liu, *Anal. Chem.*, 60 (1988) 173.
31 K. W. Sigvardson, J. M. Kennish and J. W. Birks, *Anal. Chem.*, 56 (1984) 1096.
32 W. A. MacCreham and W. E. May, *Anal. Chem.*, 56 (1984) 625.
33 W. A. MacCreham, S. D. Yang and B. A. Benner, Jr., *Anal. Chem.*, 60 (1988) 284.
34 W. A. MacCreham, W. E. May, S. D. Yang and B. A. Benner, Jr., *Anal. Chem.*, 60 (1988) 194.
35 S. B. Tejada, R. B. Zweidinger and J. E. Digsby, Jr., *Anal. Chem.*, 58 (1986) 1827.
36 S. M. Rappaport, Z. L. Jin and X. B. Xu, *J. Chromatogr.*, 240 (1982) 145.
37 A. Robbat, Jr. and T. Y. Liu, *J. Chromatogr.*, (1990) in press.
38 P. J. Doherty, *Master Thesis*, Tufts University, Medford, MA, 1985.
39 A. Robbat, Jr. and N. P. Corso, *U.S. Pat.*, No. 4 801 430 (1989).